In situ mechanical testing of templated carbon nanotubes

Shaoning Lu, Zaoyang Guo,[a] Weiqiang Ding, and Dmitriy A. Dikin
Department of Mechanical Engineering, Northwestern University, 2145 Sheridan Road, Evanston, Illinois 60208-3111

Junghoon Lee
School of Mechanical and Aerospace Engineering, Seoul National University, San 56-1 Shilim, Kwanak, Seoul 151-742, Korea

Rodney S. Ruoff[b]
Department of Mechanical Engineering, Northwestern University, 2145 Sheridan Road, Evanston, Illinois 60208-3111

(Received 10 July 2006; accepted 28 August 2006; published online 13 December 2006)

A new microelectromechanical system (MEMS)-based tensile testing stage (with integrated actuator, direct load sensing beam, and electrodes for controlled assembly of an individual nanostructure) was developed and used for *in situ* tensile loading of a templated carbon nanotube (T-CNT) inside a scanning electron microscope (SEM). Specifically, an increasing tensile load was applied to the T-CNT by actuating the device and high-resolution scanning electron microscopy images were acquired at different loads. The *load* (from the bending of the direct force-sensing beam), the *elongation* of the specimen during loading, and the *specimen geometry* were all obtained from analysis of SEM images. The stress versus strain curve and Young's modulus were thus obtained. A model is presented for the tensile loading experiment, and the fit value of Young's modulus from this model is compared to values obtained by an independent method. The results of this experiment on a T-CNT suggest the use of this device for loading other nanostructures and also for designing other MEMS-based systems, such as a compressive testing stage. © *2006 American Institute of Physics.* [DOI: 10.1063/1.2400212]

I. INTRODUCTION

The mechanics of nanostructures are of intrinsic and practical interest. Example approaches for studying mechanical properties of nanostructures include nanoindentation,[1] tensile loading experiments with atomic force microscopy (AFM) cantilevers,[2–5] and bending or rolling on substrate surfaces using scanning tunneling microscopy (STM)/AFM tips.[6,7] Here, we report a microelectromechanical system (MEMS) testing stage with integrated actuators, force-sensing structures, and electrodes for assembly of nanostructures. A useful feature of MEMS-based testing stages is versatility of design and fabrication, and that they can be mass manufactured. Recently, MEMS have been used as a testing tool for probing mechanics, such as for actuators or force sensors.[8–12]

Configuring nanostructures on MEMS devices is challenging. Thin Al films have been tested in a MEMS force-sensing device.[12] One typical approach was to use a manipulator to first pick up and then transfer nanostructures onto the MEMS device.[13–15] Direct growth of nanostructures such as carbon nanotubes (CNTs) on MEMS has also been achieved.[16,17] However, the chemical vapor deposition process used in the growth limits the types of materials that the MEMS device can be made of.[18] At this time, mounting nanostructures on MEMS devices, particularly those having moving components, remains a significant challenge.[19]

We present a new MEMS device composed of an actuation unit, direct force-sensing beams, and integrated electrodes for dielectrophoretic deposition of nanostructures. The device has been successfully used to conduct tensile testing on *templated carbon nanotubes* (T-CNTs) in a scanning electron microscope (SEM). Single T-CNTs were assembled onto the device across the testing platforms by electric field guided assembly as will be described further below. A "fountain pen-like" writing technique with a glass micropipette was used to deposit a small amount of paraffin material on top of the suspended platforms at a distance less than 30 μm from the T-CNT, to speed up the electron beam induced deposition (EBID) process of making clamps. An increasing tensile load was applied to the T-CNTs and the magnitude of the load was obtained from the bending of the force-sensing beam, analyzed from SEM images. By fitting the stress-strain curve a modulus of 14.6±4.6 GPa was obtained for the T-CNT. These T-CNTs are known to be amorphous and probably contain hydrogen.[20] The experimental methods were confirmed by a theoretical model, and also by measurement of other T-CNTs by another method involving independently manipulated AFM cantilevers.

II. DESIGN AND FABRICATION OF THE SEM TESTING STAGE

Figure 1 shows the SEM image of our MEMS device. This device is designed with three levels of functionality: mechanical structure, electrical circuit, and thermal path.

[a]Present address: Departments of Mechanical and Civil Engineering, University of Glasgow, Glasgow G12 8LT, Scotland, UK.
[b]Author to whom correspondence should be addressed; FAX: 847-491-3915; electronic mail: r-ruoff@northwestern.edu

The *mechanical structure* includes an actuation unit, two supporting beams [to attach platform A, Fig. 1], and two direct force-sensing beams (with platform B). The actuation unit is composed of thermal expansion beams and a motion amplification mechanism. By running current through the thermal expansion beams, displacement at their free ends [end bar in Fig. 1(a)] is transferred into nanoscale motion along the axis of the platform A [OO′ in Fig. 1(b)] by a V-shaped structure for motion amplification.[10] On the opposite side of platform A, platform B is attached in the middle of the direct force-sensing beam, which is suspended and clamped at both ends to the fixed contact pads (Ω1 and Ω3). In typical use, the specimen (here, a T-CNT) would be mounted and clamped across platforms A and B. When loading the specimen with the actuation unit, the force applied can be measured from the deflection of the direct force-sensing beam. Such an approach has the flexibility to separate the electrical circuits for assembly and testing in the same device.

The *electrical circuit* has three parts: (i) the contact pads for introducing electrical current into the silicon structure (the contact pads contain the silicon base and metal films), (ii) the silicon structure itself as the Joule heating element (overlaps the thermal expansion beams of the *mechanical actuation unit*), and (iii) the electrical path for electric field-assisted deposition of nanowires such as T-CNTs (dielectrophoretic deposition), including the metal electrodes on the two opposing platforms [A and B, Fig. 1(b)] and the conductive silicon structures. The platforms A and B are fabricated such that they are electrically isolated from each other, so that an electric field can be applied between A and B through the large contact pads P2 and Ω2 on the silicon base. The shape of the platforms (and electrodes) is optimized for controlled deposition of nanowires, for a high aspect ratio Si structure. After T-CNT assembly, pads Ω1, Ω2, and Ω3 are electrically connected to achieve equal potential across the T-CNT (Ω3 is in a position symmetric to Ω1, and not shown in Fig. 1). To prevent any short circuit among the silicon structures occurring through the substrate, the device was fabricated in a silicon wafer bonded to a Borofloat® glass wafer. The *thermal path* is created such that the heat is generated in the thermal expansion beams and dissipated to the large silicon base of the contact pads through the supporting beams (the two suspended thin beams attached on each side of the platform A). Such a layout ensures that the actuator retracts platform A away from platform B.[21]

Finally, a reservoir for liquid runoff was designed to enclose the entire device, for the electric-field guided assembly.

The device was fabricated in silicon-on-glass made through the anodic bonding process. A 3 in. double side polished (DSP) wafer (*P* type, 0.02 Ω-cm, 100 μm thick, KMBH Associates) was used as the structure layer, and bonded to a 4 in. DSP Borofloat® glass (Mark Optics) using the EV501 bonder (EV group). Electrodes were first patterned by photolithography (S1818, Shipley), metal evaporation (Cr 10 nm and Au 100 nm) with a CVC SC4500 evaporator, followed by a lift-off process. A second 3.7 μm thick layer of photoresist (SPR 220-3.0, Shipley) was then coated to pattern the silicon structure and also served as an etching

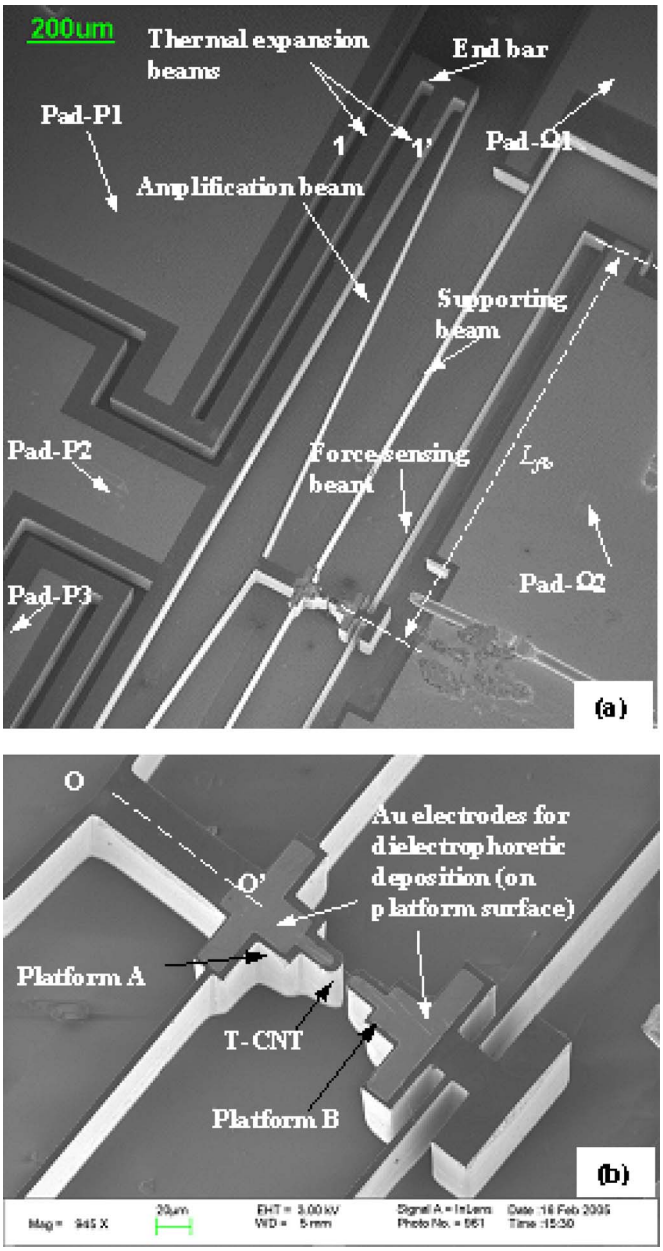

FIG. 1. (a) SEM image of a MEMS-based testing device with direct force-sensing beams. (b) Central area of the testing platforms, with a T-CNT deposited across the gap.

mask for the deep reactive ion etching (DRIE) process (Unilever axis 770). The device layer silicon was etched through until etching stopped at the glass surface. Each individual device was cut off from the bonded wafer, and the freestanding silicon structure was released by timed hydrofluoric acid etching (49%, Fisher Scientific). The remaining photoresist was then removed by Nanostrip (Cyantek Corporation). The device was finally rinsed with absolute alcohol (200 Proof, Pharmco Products, Inc.) to thoroughly clean the device, followed by drying.

III. ASSEMBLY OF TEMPLATED CARBON NANOTUBE (T-CNT) AND INSTRUMENTATION OF THE DEVICE

Due to the challenges and difficulties associated with direct growth of CNTs at high temperature on MEMS

devices,[18,22] we used the electric field-guided assembly method (dielectrophoretic deposition) to assemble a single T-CNT onto the device from a liquid dispersion, as reported in our previous work.[23] For the current MEMS device, the design layout of the mechanical structure and electrode shape (and size) was optimized to maximize the uniformity of the electric field. The electrical signal was experimentally determined to minimize the interference from the surrounding Si structures around platforms A and B. A composite electrical signal with a 20 V_{pp} ac (f=5 MHz, Agilent 33120A function generator) and a 1.5 V dc (Agilent 6544A dc power supply) bias was applied to the two Au contact pads [P2 and Ω2 in Fig. 1(b)]. Approximately 14 μl of T-CNT/ethanol dispersion (T-CNT in 100% ethanol) was dropped onto the device while the electric field was on. (The volume of the droplets should not exceed the reservoir volume surrounding the device.) The deposition was conducted on a probe station equipped with an optical microscope (Bausch & Lomb MicroZoom™) and a charge-coupled device (CCD) video camera (Hitachi HV-C20M). The deposition process was monitored on a TV screen connected to the CCD camera. Since the silicon is conductive, the electric field is mostly concentrated between the A and B platforms. During the deposition process, the T-CNTs were attracted and aligned across the Au coated surfaces of the platforms. (This was due to the native oxide coating on the exposed silicon surface beyond the gold and remaining polymer on the sidewall from the Bosch etching process.[23]) The power was manually turned off about 30 s after a deposition of one T-CNT. The device was then dried in a critical point dryer (Polaron E3000), as described previously.[23]

The MEMS device with the T-CNT assembled was then glued to a chip carrier (LDCC 28-pin leaded chip carrier, Spectrum Semiconductor Materials, Inc.). The electrical connection between the contact pads of the MEMS device and the chip carrier was made by wire bonding (West Bond Model 7400E). Pads Ω1, Ω2, and Ω3 were also connected with wire bonding. This assembly could then be mounted on a regular SEM sample stub with proper insulation between the pins of the LDCC chip carrier. Electrical signals were introduced through an electrical feedthrough (flange) on the SEM.

To perform tensile loading experiments, it is necessary to first clamp the T-CNT to the two platforms because the interaction between the T-CNT and substrate surface is not strong enough for loading the T-CNT. (We observed T-CNTs sliding on the testing stage without application of any adhesive or other clamps when the testing stage was actuated.) One method for making clamps is via electron beam induced deposition (EBID), which is a process of using an electron beam to decompose molecules and thereby deposit material on the surface region exposed to the e-beam. It is an effective method for fabricating local electrodes for transport measurements or clamps to hold one dimensional nanostructures, such as nanotubes, nanowires, or nanorods, for mechanical or electrical testing.[3,4,24–27] The EBID process in a standard SEM relies on the residual hydrocarbon in the vacuum chamber, thus the deposition is relatively slow. It is challenging to fabricate strong enough clamps for testing (to fracture) T-CNTs of 200–400 nm diameter. To accelerate the clamping process we introduced a solid phase hydrocarbon source (paraffin) near the T-CNT. The greatly increased deposition rate, and the composition and mechanical properties (strength) of the EBID clamp from such a precursor have been discussed in our previous work.[28]

From trial tests we learned that the paraffin should be placed within 20 μm of the desired area for rapid clamp deposition. The amount of paraffin material was limited by the surface size of each platform, thus it must be within an area less than 20×40 μm^2. We developed a method to make an EBID deposit on the free-standing platform attached to the suspended microbeam that avoids breaking the suspended beam or wiping off the T-CNT. As mentioned, a glass micropipette was fabricated for delivering the paraffin from a liquid solution to the desired location. This is similar to the "nano-dispenser" and dip-pen lithography approaches that have also exploited a capillary bridge between a "fountain pen" writing element and the substrate.[29,30] The paraffin was first dissolved in a liquid solution [5% weight paraffin dissolved in toluene; the paraffin used here was 99% n-hexacosane $(CH_3CH_2)_4CH_3$;Alfa Aesar]. The glass fountain pen with a tapered and sharp nozzle [at the tip, outside diameter (o.d.) ~10 μm and inside diameter (i.d.) ~5 μm] was fabricated using a borosilicate glass pipette having uniform diameter (o.d. 1.0 mm, i.d. 0.58 mm, 10 cm length, Warner Instrument Corp., Cat. No. G100-4). The pipette was pulled with a vertical pipette puller (David Kopf Instruments, model 700C) until it broke, which produced a tapered section along the axis of the glass pipette. This section was much more compliant than the beam structure of the MEMS device, so it did not break any silicon structures when touching the platforms and microbeams. The solution was injected into the glass pen (micropipette) from the wider end with a loading pipette (the loading pipette can be made by pulling, for example, the Fisher brand disposable soda-lime glass Pasteur pipette). The liquid solution was then pushed through the narrow orifice of the micropipette by using a FemtoJet device (Eppendorf, parameters: p_i=880 hPa, t_i=1–3 s, p_c=30 hPa). After a small amount of paraffin solution was pushed out of the narrow nozzle of the glass fountain pen, the toluene evaporates immediately, leaving a minute amount of paraffin deposit at the outer surface of the nozzle tip. Once this paraffin deposit is formed, the micropipette is removed from the FemtoJet unit and attached to a probe holder on the probe station to perform the deposition on the MEMS testing stage.

The process was monitored with the same optical microscope mentioned above. The probe holder has three degrees of freedom so that the pipette nozzle could be positioned close to that end of the T-CNT in contact with the platform. Once the nozzle was brought into contact with the top surface of platform A or B, the paraffin solution was drawn out of the pipette by the capillary force (between the paraffin cluster, edge of the pipette nozzle, and the stage surface) and also by wetting by the surface. The toluene rapidly evaporates, leaving paraffin on the surface near the T-CNT.

After the paraffin is deposited on each platform near the ends of the specimen, the device was transferred into the

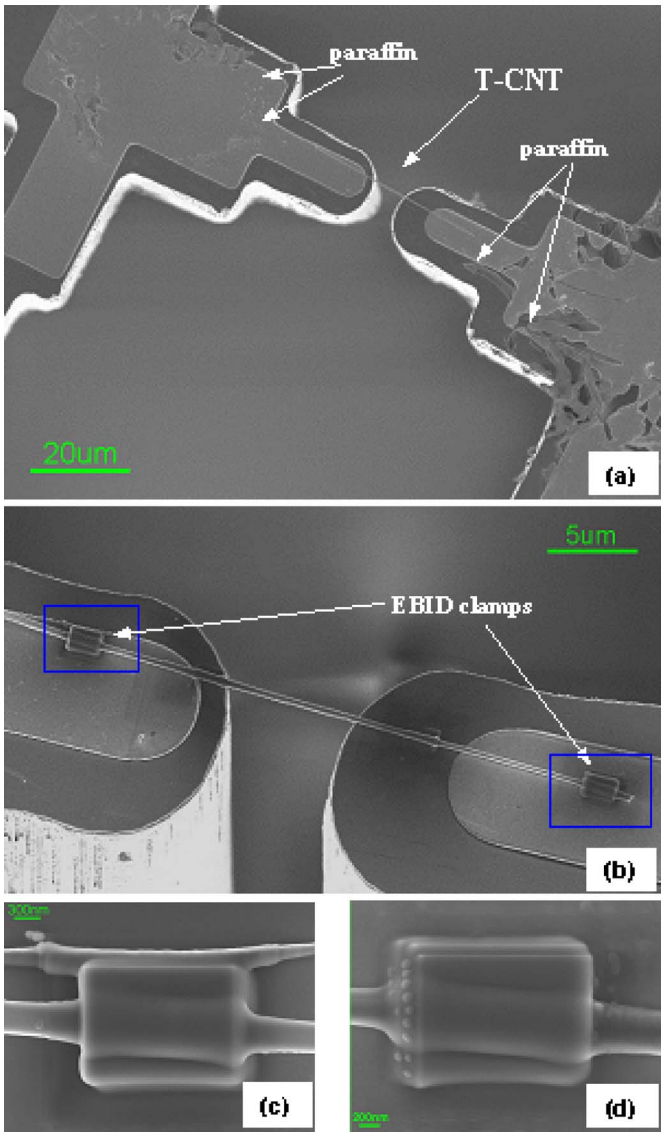

FIG. 2. (a) A SEM image of a T-CNT deposited across the platforms before being clamped. Paraffin has been deposited close to each end of the T-CNT on each of the platforms. (b) The T-CNT after clamp deposition by the EBID/paraffin method. (c-d) Magnified views of each EBID deposit on each end of the T-CNT.

SEM for clamp fabrication. Figure 2(a) shows an SEM image of such a device, with a T-CNT deposited across the two platforms and with paraffin nearby. The clamps were fabricated by scanning a small region such that the T-CNT end was located at the center of the scanned area, with the SEM electron beam at a magnification in the range of 100 000–120 000. The clamp was typically 1–1.4 μm long and 0.7–1 μm wide. The time needed to fabricate such a (comparatively) large clamp varied from 10 to 30 min, depending on the distance and the quantity of the paraffin nearby. Figure 2(b) is an enlarged view of the T-CNT in Fig. 2(a) after clamping. A close-up view of each clamp is shown in Figs. 2(c) and 2(d).

IV. MECHANICAL TESTING AND ANALYSIS OF THE RESULTS

After deposition of the carbonaceous clamp material by EBID, the T-CNT was then tensile loaded. A device with the same dimensions as shown in Fig. 1 was used. The resistance of the thermal expansion beams on each side of the central electrode was 86.4 Ω [beams 1 and 1' in Fig. 1(a)]. The resistivity was 0.02 Ω cm, as determined with a four-point probe method and the dimensions measured from SEM images. The total resistance of the entire device including the electrical wires and soldering joints was about 45 Ω. The testing was carried out in the vacuum chamber of a LEO 1525 SEM ($\sim 10^{-4}$ Pa) with the dc current applied on the MEMS device and incremented in 10 mA steps. The voltage drop across the device was simultaneously recorded to obtain the supplied power. With the current running through the thermal expansion beams, the actuation unit (as defined above) retracts platform A away from platform B, which applies a tensile load to the T-CNT.

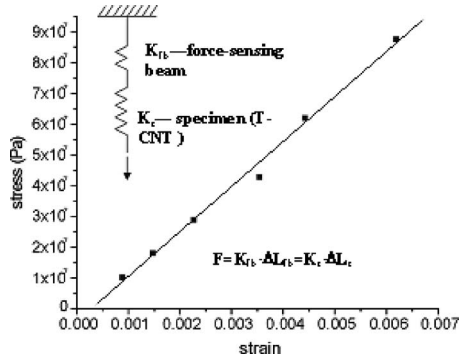

FIG. 3. Stress vs strain data for a T-CNT loaded with the MEMS device having the design shown in Fig. 1. K_b is the spring constant of the force-sensing beam, ΔL_{fb} is the displacement of the beam, K_s is stiffness of the specimen (T-CNT), and ΔL is the elongation of the specimen.

The gauge length of the T-CNT (chosen as the length between the inner edges of the two clamps) was measured from SEM images, usually at a magnification in the range 25 000–36 000. Strain was computed from the original length and the measured length during loading. The force on the T-CNT was calculated by $F=K_{\mathrm{fb}}\Delta x_{\mathrm{fb}}$, where Δx_{fb} is the deflection of the force-sensing beam and K_{fb} is the beam stiffness. The deflection of the force-sensing beam is obtained by measuring the displacement of platform B attached at the center of the force-sensing beam. A spring diagram that represents the force-sensing beam and the specimen (T-CNT) is shown in the inset of Fig. 3. From the equilibrium of forces, the load on the T-CNT from the actuator is equal to the force that the T-CNT applies on the force-sensing beam. The stiffness of the force-sensing beam was calculated from $K_{\mathrm{fb}}=24EI_{\mathrm{fb}}/L_{\mathrm{fb}}^3$, where the silicon modulus E for the (110) direction [169 GPa (Ref. 31)] is used, since the device is fabricated such that the long edge of the beam was along the (110) direction. I_{fb} is the moment of inertia of the beam, and L_{fb} is the length from the center of the beam (at platform B) to one of the fixed ends, as in Fig. 1(a).

The diameters of the T-CNTs were measured in the SEM. As the T-CNT sample was synthesized by pyrolyzing ethylene in an alumina nanopore membrane, the T-CNT diameters mimic the i.d. of each of the pores in the membrane, and we have found that the T-CNTs that we made[20] were not uniform along their entire length. Such T-CNTs also are amorphous in structure.[20] An average diameter was used to

calculate the cross sectional area. For the particular T-CNT tested, the average outer diameter was 344 nm,[32] and the average inner diameter was assumed to be half the outer diameter, as observed from the open ends of the T-CNT projecting past the clamps. With these values chosen for the (assumed average) geometry, a "stress" in the T-CNT can be calculated and plotted against the strain, as shown in Fig. 3. Young's modulus, based on these assumptions, was obtained from a linear fit of the stress-strain curve, yielding 14.6±4.6 GPa for this T-CNT. This value is discussed further below. (We also emphasize that the primary focus of this article is a report of the development of a new device and also useful approaches for attaching nanowires and nanotubes to such types of devices, for their tensile loading. Future studies will involve testing more uniform nanowires; the somewhat nonuniform T-CNTs were chosen due to their size, which made their observation by standard light microscopy straightforward.)

The device was further analyzed with a theoretical model developed by Lu *et al.*[21] This model was used to obtain the stiffness of the T-CNT from the displacement of platform A with a load from the supporting beam only, versus with a different magnitude of load when a T-CNT is attached to the fixed platform, as

$$K_{\mathrm{su}} = \frac{(K_d + K_b)(x_1 - x_2)}{x_2}. \tag{1}$$

Here K_{su}, K_d, and K_b are the stiffness of the *specimen* (*T-CNT*) *unit*, the *actuation unit*, and the *supporting beam*, respectively. The stiffness of a "unit" is defined as the force required for the unit to have a unit displacement in a particular direction. For the specimen, $K_{\mathrm{su}}=A_sE_s/L_s$ and x_1 is the displacement of platform A without a T-CNT attached, while x_2 is the displacement of platform A with a T-CNT attached.

To apply this model for the new device used here, we consider the T-CNT (K_s) and the direct force-sensing beam (K_{fb}) as one specimen unit (with stiffness K_{su}). We also define a *measurement unit* composed of the specimen unit and the supporting beam. When actuating the device without a T-CNT assembled, the load applied on the actuation unit is only from the supporting beam (K_b). With the T-CNT present, the load will be from the entire measurement unit. Hence, Eq. (1) becomes

$$K_{\mathrm{su}} = \frac{(K_d + K_b)(x_1 - x_2)}{x_2} = \frac{1}{1/K_s + 1/K_{\mathrm{fb}}}, \tag{2}$$

and the stiffness of the specimen (T-CNT) is

$$\frac{1}{K_s} + \frac{1}{K_{\mathrm{fb}}} = \frac{x_2}{(x_1 - x_2)} \cdot \frac{1}{(K_d + K_b)}$$

$$\Rightarrow K_s = \frac{(x_1 - x_2)(K_d + K_b)K_{\mathrm{fb}}}{x_2 K_{\mathrm{fb}} - (x_1 - x_2)(K_d + K_b)}, \tag{3}$$

K_{fb}, K_d, and K_b can be obtained from finite element analysis (FEA) by using programs such as ABAQUS with the actual beam dimensions as measured in the SEM.

The FEA simulation shows that the theoretical value of $(x_1-x_2)/x_2$ is 0.0071. From the experimental results presented above, we already have the displacement x_2 with the load from the sample unit. To obtain the displacement x_1 with load from the supporting beam only, we cut the T-CNT by focused ion beam milling (Hitachi FIB 2000A) and measured the displacement of platform A (x_1) while operating the device at 65.6 mW. The value of $(x_1-x_2)/x_2$ from this experiment was ≈0.0097. This non-zero difference between the theoretical and measured values may be due to the measurement resolution (~4.0 nm pixel resolution at 100 000× magnification). In this case, to detect $(x_1-x_2)/x_2$ as small as the theoretical value of 0.0071 with a displacement x_1 on the order of 300 nm (for example, for the 65.6 mW power input), the difference of (x_1-x_2) should be ~3.0 nm, beyond the accuracy of our measurement.

Denoting the displacement of the force-sensing beam as x_3 (also as Δx_{fb} in the above analysis), the elongation of the T-CNT is (x_2-x_3). Alternatively, the specimen's stiffness K_s can also be obtained from the force and its elongation directly from

$$K_s = \frac{F}{x_2 - x_3} = \frac{x_3 K_{\mathrm{fb}}}{x_2 - x_3}. \tag{4}$$

There are two approaches for obtaining a higher accuracy measurement of K_s: (i) to enlarge the elongation $(x_2$-$x_3)$ of the specimen, which requires an increase in the stiffness of the force-sensing beam (K_{fb}, since x_3 should decrease), (ii) to achieve a more accurate reading of the force applied on the specimen (for the same load, a larger deflection x_3 thus a more compliant force-sensing beam, equivalently less stiffness). As often occurs, there are factors that "trade-off" in trying to find the optimal design. Preferably, the stiffness of the force-sensing beam (K_{fb}) should be of the same order as that of the specimen (K_s). (One seems to need to prior knowledge of what one is attempting to measure.) For a nanowire with unknown mechanical properties a device without the direct force-sensing beam can be used for preliminary testing. Based on this preliminary value and the above equations, the device design can be optimized to have a direct force-sensing beam of proper stiffness to provide better results, yielding more accurate stress versus strain data.

The force-displacement response of similar T-CNTs was measured with a home-built nanomanipulator to compare with the results from the MEMS testing stage. The method of using AFM cantilevers for tensile loading was employed, as was used for testing multiwalled carbon nanotubes and carbon nanocoils.[3,4,33] T-CNTs from the same fabrication run were clamped between two opposing AFM cantilever tips (NSC12 k=0.3 N/m and k=14.0 N/m, MikroMasch, Inc.) with the EBID method. A tensile force was applied to the T-CNT by displacing the soft cantilever with voltage applied to a piezoelectric bimorph component. The relatively compliant cantilever was used as the force-sensing element and its deflection was obtained from the recorded SEM images, as were the values of elongation of the T-CNT at each separate load. The moduli obtained for two T-CNTs were 16±2 and 30±12 GPa, respectively. As mentioned, these T-CNTs have an amorphous structure,[20] so the modulus obtained from using the MEMS testing device is in the right range for the amorphous carbon that they are comprised of. We note

that the T-CNTs may possibly contain hydrogen, that is, might be composed of hydrogenated amorphous carbon.

V. DISCUSSION

In summary, a MEMS-based tensile testing stage was developed, with integrated actuator, direct load sensing beam, and circuits for assembling an individual nanostructure, and the capability for *in situ* mechanical testing on individual templated carbon nanotubes (T-CNTs) in SEM was demonstrated. The device provides well-controlled nanoscale displacement and force for loading nanostructures. Novel approaches have been developed to align and mount an individual T-CNT across the two opposing platforms of the testing stage. A fountain-pen writing technique was developed to deposit paraffin for rapid clamping of the T-CNT in the SEM by electron beam induced deposition.

Tensile tests were performed on the T-CNT with the MEMS testing stage. The load was obtained from the deformation of the direct force-sensing beam and the strain was calculated from the recorded SEM image by pixel counting. Young's modulus was obtained from a linear fit of the stress-strain curve. The fit value for the modulus of the T-CNT is evidently due to its atomic structure and composition. Based on a previous model, an experiment was conducted by cutting off the T-CNT, to verify the testing results. Independent tests of the stiffness of such T-CNTs were performed with a home-built nanomanipulator for comparison.

The experiments suggest the potential use of this MEMS testing stage for tensile testing on a variety of nanowires and nanotubes. Suggestions on optimizing the design and how to use the device, based on the theoretical simulation and the testing results, were presented for future testing of new nanostructures with unknown properties. Finally, the current modular design approach of defining different functional units, such as an actuation unit, measurement unit, and sample unit, provides flexibility, such as for design of a compressive testing stage.

ACKNOWLEDGMENTS

The authors appreciate the support from the NSF (CMS-0304506; NIRT: Synthesis, Characterization and Modeling of Aligned Nanotube Arrays for Nanoscale Devices, Ken Chong program manager) and the Naval Research Laboratory (Grant No. N00173-04-2-C003). The fabrication work was performed in part at the Cornell Nano-Scale Science & Technology Facility (a member of the National Nanofabrication Users Network), which is supported by the National Science Foundation under Grant No. ECS-9731293, its users, Cornell University, and industry affiliates. Scanning electron microscopy and focused ion beam machining were done at the Northwestern University Atomic and Nanoscale Characterization Experimental Center.

[1] S. A. S. Asif, K. J. Wahl, R. J. Colton, and O. L. Warren, J. Appl. Phys. **90**, 1192 (2001).
[2] M. F. Yu, M. J. Dyer, G. D. Skidmore, H. W. Rohrs, X. K. Lu, K. D. Ausman, J. R. Von Ehr, and R. S. Ruoff, Nanotechnology **10**, 244 (1999).
[3] M. F. Yu, B. S. Files, S. Arepalli, and R. S. Ruoff, Phys. Rev. Lett. **84**, 5552 (2000).
[4] M. F. Yu, O. Lourie, M. J. Dyer, K. Moloni, T. F. Kelly, and R. S. Ruoff, Science **287**, 637 (2000).
[5] M. F. Yu, B. I. Yakobson, and R. S. Ruoff, J. Phys. Chem. B **104**, 8764 (2000).
[6] M. R. Falvo, G. J. Clary, R. M. Taylor, V. Chi, F. P. Brooks, S. Washburn, and R. Superfine, Nature (London) **389**, 582 (1997).
[7] L. M. Bellan, J. Kameoka, and H. G. Craighead, Nanotechnology **16**, 1095 (2005).
[8] J. Brugger, V. P. Jaecklin, C. Linder, N. Blanc, P. F. Indermuhle, and N. F. de Rooij, J. Micromech. Microeng. **3**, 161 (1993).
[9] J. J. Yao, S. C. Arney, and N. C. MacDonald, **1**, 14 (1992).
[10] S. Lu, D. D. Dikin, S. Zhang, F. T. Fisher, J. Lee, and R. S. Ruoff, Rev. Sci. Instrum. **75**, 2154 (2004).
[11] M. T. A. Saif, S. Zhang, M. A. Haque, and K. J. Hsia, Acta Mater. **50**, 2779 (2002).
[12] M. A. Haque and M. T. A. Saif, Exp. Mech. **42**, 123 (2002).
[13] M. A. Haque and M. T. A. Saif, Sens. Actuators, A **97–98**, 239 (2002).
[14] Y. Zhu, N. Moldovan, and H. D. Espinosa, Appl. Phys. Lett. **86**, 013506 (2005).
[15] A. B. Hartman, P. Rice, D. S. Finch, G. D. Skidmore, and V. M. Bright, *Force-Deflection Characterization of Individual Carbon Nanotubes Attached to MEMS Devices* (IEEE, Maastricht, The Netherlands, 2004), pp. 426–429.
[16] B. Babic, J. Furer, S. Sahoo, S. Farhangfar, and C. Schönenberger, Nano Lett. **3**, 1577 (2003).
[17] N. R. Franklin, Q. Wang, T. W. Tombler, A. Javey, M. Shim, and H. Dai, Appl. Phys. Lett. **81**, 913 (2002).
[18] Y. Zhang *et al.*, Appl. Phys. Lett. **79**, 3155 (2001).
[19] K. Hoshino, Y. Murakami, S. Maruyama, K. Matsumoto, and I. Shimoyama, *Electrostatically-actuated micro cantilevers for electromechanical measurement of single-walled carbon nannotubes grown by catalytic CVD*, 17th IEEE International Conference on Micro Electro Mechanical Systems, Maastricht, 2004, pp. 446–449.
[20] T. T. Xu, F. T. Fisher, L. C. Brinson, and R. S. Ruoff, Nano Lett. **3**, 1135 (2003).
[21] S. Lu, Z. Y. Guo, W. Q. Ding, and R. S. Ruoff, Rev. Sci. Instrum. **5**, 77 (2006).
[22] A. M. Cassell, N. R. Franklin, T. W. Tombler, E. M. Chan, J. Han, and H. Dai, J. Am. Chem. Soc. **121**, 7975 (1999).
[23] S. Lu, J. Chung, and R. S. Ruoff, Nanotechnology **16**, 1765 (2005).
[24] L. Dong, F. Arai, and T. Fukuda, Appl. Phys. Lett. **81**, 1919 (2002).
[25] D. N. Madsen, K. Mølhave, R. Mateiu, A. M. Rasmussen, M. Brorson, C. J. H. Jacobsen, and P. Bøggild, Nano Lett. **3**, 47 (2003).
[26] G. Boero *et al.*, Appl. Phys. Lett. **86**, 042503 (2005).
[27] P. Bøggild, T. M. Hansen, C. Tanas, and F. Grey, Nanotechnology **12**, 331 (2001).
[28] W. Ding, D. A. Dikin, X. Chen, R. D. Piner, X. Wang, X. Li, R. S. Ruoff, and E. Zussman, J. Appl. Phys. **98**, 014905 (2005).
[29] A. Meister, M. Liley, J. Brugger, R. Pugin, and H. Heinzelmann, Appl. Phys. Lett. **85**, 6260 (2004).
[30] R. D. Piner, J. Zhu, F. Xu, S. Hong, and C. A. Mirkin, Science **283**, 661 (1999).
[31] J. J. Wortman and R. A. Evans, J. Appl. Phys. **36**, 153 (1965).
[32] The diameter along the T-CNT was not constant. It was measured from SEM images and averaged (with four measurement points: one near the inner edge of each clamp, one at the thinnest cross section, and one between the thinnest point and one inner edge of clamp). The average cross sectional area A_s is 6.97×10^{-14} m^2.
[33] X. Chen, S. Zhang, D. A. Dikin, W. Ding, and R. S. Ruoff, Nano Lett. **3**, 1299 (2003).